



Published in final edited form as:

*Med Phys.* 2008 January ; 35(1): 301–309. doi:10.1118/1.2821702.

## Endovascular image-guided interventions (EIGIs)

Stephen Rudin<sup>a)</sup>, Daniel R. Bednarek<sup>b)</sup>, and Kenneth R. Hoffmann<sup>c)</sup>

*Toshiba Stroke Research Center, University at Buffalo, State University of New York, Biomedical Research Building, Room 445, 3435 Main Street, Buffalo, New York 14214*

### Abstract

Minimally invasive interventions are rapidly replacing invasive surgical procedures for the most prevalent human disease conditions. X-ray image-guided interventions carried out using the insertion and navigation of catheters through the vasculature are increasing in number and sophistication. In this article, we offer our vision for the future of this dynamic field of endovascular image-guided interventions in the form of predictions about (1) improvements in high-resolution detectors for more accurate guidance, (2) the implementation of high-resolution region of interest computed tomography for evaluation and planning, (3) the implementation of dose tracking systems to control patient radiation risk, (4) the development of increasingly sophisticated interventional devices, (5) the use of quantitative treatment planning with patient-specific computer fluid dynamic simulations, and (6) the new expanding role of the medical physicist. We discuss how we envision our predictions will come to fruition and result in the universal goal of improved patient care.

### Keywords

endovascular; image-guided intervention; detectors; cone beam CT; computer fluid dynamics (CFD)

### I. Introduction

The three greatest killers in the developed world are heart disease, cancer, and stroke or neurovascular disease, with the last being the greatest cause of disability. After drug treatment, the primary interventional therapy for vascular diseases and an important treatment modality for cancer are endovascular image-guided interventions (EIGIs). EIGIs generally involve the insertion of a catheter into the femoral artery, which is then threaded under fluoroscopic guidance through the vasculature to the site of the pathology to be treated. The pathology may be a portion of a vessel that is stenosed, or totally occluded, either by chronic plaque formation or by acute clot localization. The pathology may also be a portion of a vessel that is weakened and bulges to form an aneurysm, which may hemorrhage. Finally, it may be a hypervascular region such as a tumor bed or an arteriovenous malformation. The EIGI may involve delivery of a drug or embolic material through the catheter, or may be the delivery of a device such as a stent that may be used to keep a stenosed vessel open. During the course of the intervention, rapid-sequence fluoroscopic x-ray imaging is usually relied on for guidance.

Increasingly, EIGIs are replacing invasive surgical procedures because of the reduced mortality, morbidity, and discomfort to the patient.<sup>1</sup> For example, surgical clipping of aneurysms, which just a few years ago was the standard of care, is now being replaced by the deployment of embolic material, such as detachable coils delivered through a catheter under

<sup>a)</sup>Author to whom correspondence should be addressed. Electronic mail: E-mail: srudin@buffalo.edu.

<sup>b)</sup>Electronic mail: bednarek@buffalo.edu

<sup>c)</sup>Electronic mail: kh9@buffalo.edu

fluoroscopic guidance into the aneurysm, thus replacing an invasive external approach most likely through the skull with a minimally invasive endovascular intervention.<sup>2–4</sup> In this work, we will discuss the basic features and current status of EIGI in terms of the imaging system, radiation dose, interventional equipment and devices, procedure characteristics and treatment planning, and personnel involved. We will first give an overview of the current state of EIGI and then make predictions about each feature category, providing the rationale and evidence for each prediction and the strategy we suggest for making each forecast become a reality in a 7–10 year time frame.

## II. Current Status

Before an EIGI procedure is scheduled, diagnostic procedures to find and analyze the pathological region are done preferably using noninvasive imaging modalities, such as multislice computed tomography (MSCT) or magnetic resonance imaging (MRI), and followed up by higher-resolution minimally invasive angiographic procedures done in dedicated angiographic or special procedure x-ray suites.<sup>5,6</sup> Typically, EIGI procedures, if indicated, are then done under real-time x-ray image guidance in such a special procedure suite.<sup>7</sup> Thus, such a suite may be used for the initial diagnostic study and subsequently for the intervention. Rotating anode x-ray tubes, that have become more robust but have changed little in decades in overall design, are used as the source of x rays; however, dynamic x-ray detector designs are in the process of changing from the decades old x-ray image intensifier (XII) to the new flat panel detector (FPD).<sup>8</sup> The indirect FPD and the XII designs both use an x-ray absorbing structured CsI phosphor, but differ greatly thereafter. The XII converts the phosphor's light to electrons that are accelerated. This electron distribution is focused on an output phosphor to produce an intensified image of light photons and thus create a gain in brightness.<sup>9</sup> In contrast, an indirect FPD uses an array of solid state photodiodes with thin film transistor (TFT) switches and, currently, no additional gain to generate electronic signals that are directly digitized by circuitry off to the side of the x-ray sensitive region. Direct FPDs employ a photoconductor, such as amorphous selenium, to absorb the x rays and directly produce a charge, which is read out by an array of TFTs. While the XIIs have a number of disadvantages—such as glare, pincushion distortion due to the curved x-ray sensitive phosphor, S distortion due to the earth's magnetic field, and large physical volume—they have the advantages of inherently large and variable gain, adjustable magnification hence pixel size, and flexible optical output that is usable with a variety of optical image receptors or cameras.<sup>9</sup> However, the transition to FPDs for dynamic x-ray imaging has been somewhat disappointing, due to the substantial FPD additive instrumentation noise that is similar in magnitude to the signal obtained in the lower range of standard fluoroscopic exposures. This noise quantity when expressed in units of exposure may be referred to as the instrumentation noise equivalent exposure (INEE).<sup>10</sup> Other disadvantages of FPDs have been the image lag or persistence,<sup>11,12</sup> ghosting due to charge retention in the photodiode TFT array,<sup>12,13</sup> and the substantial artifacts that require corrections prior to image display. The advantages of FPDs, however, are their smaller physical size and lack of distortion, which enable improved cone-beam computed tomography (CBCT) to be accomplished with the same angiographic gantry used for the diagnostic or EIGI procedures.<sup>14</sup> For both detector systems that are currently in use, image quality may not be optimal especially in fine detail EIGIs. The details of interventional devices, such as stent struts, and small vessels, such as perforators in the brain, typically cannot be visualized because of the limited spatial resolution capabilities of current conventional detectors, although the development of some specialized CCD-based microangiographic detectors has begun.<sup>15</sup>

As EIGI procedures become more widespread and more complex, there is a continuing concern regarding lengthy procedure times and the associated radiation doses, which can be some of the highest of medical radiological studies.<sup>16,17</sup> Currently, there are dose reduction techniques available, such as spectral shaping performed automatically using selected metallic filters and

the option for reducing frame rates during fluoroscopic and angiographic acquisitions. However, other techniques, such as spatially modulating the beam for optimal dose utilization<sup>18–21</sup> and recording and displaying the details of patient dose deposition,<sup>22,23</sup> are not commonly used.

Even though EIGI procedures can be lengthy and complex, the actual EIGI devices that are used remain only somewhat more complex in design than those that were used when the field began.<sup>24</sup> Guidewires may vary in characteristics, such as torsion rigidity, flexibility, and kink resistance, due to the characteristics of the materials and windings used, and catheters may similarly vary depending upon the material and construction of the wall.<sup>25–30</sup> However, they are basically still passive cylinders and tubes that are actuated by pulling, pushing, rotating, or, in the case of balloons, inflating, all simple mechanical actions initiated at the proximal end outside the patient. Also, while devices, such as stents, and inserted material, such as embolizing coils or glues, have advanced somewhat over the years,<sup>31</sup> they are still rather simple in design and mostly passive in nature having few if any electronic, computerized, or motorized components. Even specialized active devices, such as the rotational atherectomy Rotablator (Boston Scientific Corp, Natick, MA), are basically simple rapidly rotating wires with diamond burrs at the distal tip for grinding down plaque.<sup>32</sup> Nevertheless, these mostly passive or simple devices deployed under EIGI procedures have had a major impact already in substituting for surgically invasive procedures, such as aneurysm clipping or open-heart coronary bypass procedures.

Currently, unlike in radiation therapy, quantitative treatment planning is lacking in preparation for EIGI procedures. Also, although CBCT is now available, it is not used to quantitatively plan a procedure, such as to determine in advance what guidewires, catheters, and endovascular devices can be passed through vessels using computer analysis of the mechanical properties of the vessels as well as a library of such properties for the devices combined with the derived tortuosity and other characteristics of the vessel. It is generally believed that blood flow has a major impact on the initiation of vessel pathologies,<sup>33,34</sup> as well as the outcomes of subsequent EIGIs,<sup>35,36</sup> yet there is very little done clinically to quantitatively determine the detailed flow or to predict the effect on blood flow of a proposed intervention from information gained with computer fluid dynamic (CFD) calculations in time to have any clinical impact.

Because of the present rather improvised state of clinical EIGI procedures, the personnel active during such procedures consists of a mixture of clinicians and technologists, but rarely includes medical physicists or engineers. This contrasts with radiation therapy procedures where the treatment team generally includes a medical physicist.

### III. Prediction, Evidence/Rationale, and Strategy for Implementation

We predict that in 7–10 years there will be dramatic changes in the field of EIGI procedures in all areas: Imaging equipment and doses, devices, methods of planning, as well as the role of the medical physicist. In what follows we list our predictions in each of these areas of EIGI, provide our rationale supported by evidence from current research trends, and suggest strategies for how these forecasted advances may come to fruition.

#### III.A. Imaging systems and dose

**III.A.1. Prediction 1**—Higher resolution, lower noise, and real-time image receptors—at first for the region of interest (ROI) near the intervention and then across the full field of view (FOV)—will become the standard of care for many EIGI procedures.

The rationale for this prediction is that, increasingly, MSCT and MRI are taking over the task of vascular diagnosis with angiographic special procedure rooms being devoted increasingly

to EIGI. The fact that MSCT and magnetic resonance angiography (MRA) procedures require only a venous puncture for injection of the contrast media and that image quality is improving to the point where definitive diagnoses are possible in many cases make this trend plausible. Once a diagnosis has localized the site of pathology, there may not be a need for superior image quality except over the site of the intervention. Superior resolution is needed in the ROI for both real-time fluoroscopy to actively guide the ongoing intervention and also for superior angiography to evaluate the progress of the intervention throughout the procedure and to help determine when a satisfactory endpoint has been reached.

To achieve this improvement especially over the ROI of the interventional site, either a vast improvement in current FPDs or new alternative detectors with the desired characteristics will be required. For example, large area CCDs have been considered.<sup>37</sup> Methods for reducing the effect of instrumentation noise on FPDs have been proposed; one such proposal being to provide inherently increased signal using a direct x-ray converter material having avalanche gain.<sup>38</sup> For indirect FPDs, methods include using *a*-Se avalanche photo-conductors in place of *a*-Si photodiodes<sup>39,40</sup> and placing an amplifier at each pixel of the FPD.<sup>41,42</sup> These methods enable signal amplification prior to sending the charge packet representing the signal through the TFT lines, where the noise is added and then onto the sides of the sensor where it can be amplified and digitized. Were this achievable in practice, the problem for FPDs of reducing the size of the pixels would still remain. Alternate detector designs actively being pursued by the authors consist of a high-sensitivity microangiographic fluoroscope (HSMF)<sup>10</sup> and a detector called the solid state x-ray image intensifier (SSXII). The HSMF employs a light image intensifier between the CsI phosphor and a digital videocamera with a fiber optic taper (FOT) input. This detector has a small FOV sufficient to be used for EIGI and is capable of real-time fluoroscopy as well as very-high-resolution angiography. The SSXII consists of an array of electron multiplying charge-coupled devices (EMCCDs),<sup>43,44</sup> each viewing a portion of the CsI phosphor through its own FOT coupling.<sup>45</sup> EMCCDs have all the advantages of standard CCDs: high speed, low noise, high resolution, and standard solid state production techniques. However, in addition, they have a row of hundreds of multiplying elements each with a small gain of a few percent. When cascaded together in this row, they can result in a total gain from 1 to 2000 times, depending upon the variable gain voltage setting of only around 20 V. The mosaic array of the SSXII also has the advantage of being extensible in FOV by adding modules. The INEE achievable for both such detectors is a fraction of the exposure typical of low-dose fluoroscopy, hence they have the desirable feature of being quantum limited throughout their range of operation. Additionally, unlike FPDs they have no lag or ghosting and are available with small pixel sizes. The potential advantages of SSXII and HSMF detectors compared with conventional detectors are illustrated by some examples in Figs. 1 and 2. A quantitative evaluation using linear cascade analysis<sup>46</sup> can be made of these new high-resolution detectors<sup>45,47</sup>; however, recent additions to these analytical methods will include the effects of other important factors that affect total system performance, such as focal spot blurring and scatter in the patient.<sup>48,49</sup>

**III.A.2. Prediction 2**—High-resolution CBCT will become available for the ROI of the interventional site with 3D roadmapping and automated indication of the catheter or guidewire tip superimposed.

The rationale for this prediction is that once a vascular pathology has been diagnosed, superior image quality is needed only over the site of the intervention and not over the full volume FOV. Currently, there is some effort in both academic and commercial organizations to develop 3D road-mapping capability. The syngo iPilot product<sup>50</sup> (Siemens Medical Solutions USA, Inc., Malvern, PA) or the Dynamic 3D Roadmap product<sup>51</sup> (Philips Medical Systems, N.A, Bothell, WA) are such implementations with current detector technology. Clearly, the higher the

resolution available at the interventional site, the greater the potential for a successful intervention.

To achieve this goal, higher-resolution ROI detectors, such as those in Prediction 1 above, mounted on stable detector holders added to angiographic CBCT-capable gantries will be required. The associated software will also be needed. Our group has shown that most of the artifacts due to FOV truncation (that one expects when the CT FOV is smaller than the object being imaged) can be eliminated by combining the ROI data with a lower-resolution full FOV CT image sequence. This provides sufficient information about those parts of the object that move in and out of the ROI of the projection views but which are not actually located within the ROI or volume of interest of the 3D object.<sup>52,53</sup> These high-resolution ROI-CBC images can then be used as the basis for enhanced treatment planning by calculating the simulation of the transport of a device through the vasculature<sup>53,54</sup> and for improved flow information, as will be discussed next.

**III.A.3. Prediction 3**—There will be greater accounting of patient dose distribution during EIGI with techniques to minimize integral dose as well as deterministic effects.

Although patient dose for EIGI procedures can be some of the largest of all medical procedures, it is highly nonuniform; hence, any determination of potential biological effects will depend upon a detailed knowledge of the dose distribution. Although the European Union (EU) requires the measurement of dose-area product and the International Electro-technical Commission Standard (IEC 60601–2-43, 2000) and the U.S. Food and Drug Administration (FDA) require that fluoroscopic equipment include, during the procedure, the display of air kerma rate and cumulative air kerma at an interventional reference point.<sup>55,56</sup> This is only a first step in an accurate accounting of patient dose in EIGI. A past attempt to provide more detailed patient entrance surface dose distributions in the form of a commercial product (Caregraph, Siemens Medical Systems Corp., Malvern, PA) was apparently discontinued; however, as EIGI procedures become more complex, potentially longer, and with more non-uniform dose application due to ROI techniques, recording the dose distribution will become increasingly important.

As discussed in the section on ROI-CBCT, future patient dose may be made highly nonuniform using collimation and semi-radio-opaque metallic filters.<sup>57</sup> To implement a more comprehensive dose tracking system, our group uses the digital signals available from new angiographic *c*-arm gantries, together with software that calculates and conveniently displays the cumulative entrance skin dose distribution as well as dose rate in real time.<sup>58,59</sup> This enables a clinician to obtain feedback on the consequences of their actions and to modify the procedure to reduce the risk of deterministic effects, such as erythema, epilation, and dermal necrosis.<sup>17</sup> In the future, such tracking of the beam should also be able to allow real-time accounting of effective dose and the increased risk of stochastic effects, such as cancer, which may be especially important in procedures that include exposure of the breast or thyroid.

One way to reduce the risk of entrance skin effects is to change the entrance skin exposure location and thus to “spread the surface dose”. Through determination of the 3D vasculature, future systems may guide the interventionist in selecting an optional projection to spread the dose when a deterministic threshold dose is being reached, while maintaining the needed interventional site image view to continue the procedure.

Since serious deterministic effects may not be evident until weeks after the procedure, it is important to be able to correlate the cause with the effect for proper treatment. The patient record should contain information about the distribution of dose on the skin as recommended by the FDA.<sup>60,61</sup> Using the results of a dose tracking system, the electronic medical record

will be able to log this information for future reference with the risk level indicated. The dose from subsequent procedures will be able to be added to that already recorded to provide a measure of cumulative risk. It is postulated that advances in radiobiological knowledge will allow modeling of cellular repair occurring between procedures so a more accurate estimate of cumulative risk from repeated exams can be obtained. This will further allow individual risk factors that increase radiation sensitivity (such as collagen vascular disease, diabetes mellitus, and certain pharmaceuticals and chemicals<sup>62</sup>) to be taken into account.

### III.B. Endovascular devices

**III.B.1. Prediction 4**—Endovascular devices will become finer, more patient-specific, more biocompatible, and more complex with the beginning of remotely actuated active components using shape memory alloys (SMA), micromachines, microfluidics, and microelectronics; higher-resolution imaging will be relied upon to assist in accurate device deployment.

Since minimally invasive EIGI procedures, even with the current crop of simple and somewhat passive devices, are rapidly replacing many invasive surgical procedures, it would appear to make sense that this trend would continue and be combined with advances in miniaturization. With more accurate models of a specific patient vascular pathology obtained from CBCT, more patient-specific devices can be created and deployed; however, care should be taken that new endovascular devices are designed with constituent materials that are compatible with future imaging procedures that might be required for the patient presently being treated, so there is no negative effect such as artifact generation on the images obtained.

As new more biocompatible materials are developed, devices such as bioabsorbable stents under investigation<sup>63–66</sup> should come into common usage. The initial development of remote actuation is also happening. For example, external magnetic fields are actively being used in the cardiovascular area for accurately guiding new ablation probes for electrophysiology (EP) treatment,<sup>67–69</sup> and are being proposed in the neurovascular arena for guiding the accurate deployment of new flow diversion stents [Fig. 1(D)] for treatment of aneurysms.<sup>70</sup> The use of the existing magnetic field in MRI systems is being reported for steering catheters.<sup>71</sup> There is the beginning commercial availability of remote catheter steering systems, such as the one by Hansen Medical (Hansen Medical Inc., Mountain View, CA)<sup>72,73</sup> designed for EP. However, these appear to be implemented with wires tied to external motors and hence are hard to project to the full range of EIGI, which may require navigation through a tortuous vessel. Other robotic systems have also been reported.<sup>74</sup> Remote actuation using inductive heating of shape memory polymers is also being considered.<sup>75</sup> There are also a number of new more complex devices under development for the treatment of acute ischemic stroke, such as ultrasonic clot busters, and complex catheter heads with high speed saline streams to implement suction and hence reduce clots.<sup>76</sup> New technologies in radio-frequency ablation including “software for image registration and fusion, thermal modeling, electromagnetic tracking, semiautomated robotic needle guidance, and multimodality imaging<sup>77</sup>” may also be adaptable to EIGI.

To achieve the full potential for new patient-specific, biocompatible, active EIGI devices, basic components of the process for creating these devices will have to be worked out. First, improved morphological models of the patient-specific pathology will be achieved using the high-resolution ROI-CBCT imaging methods described previously and using computer models parameterizing the desired interventional effect such as flow modification. (See, for example, the CFD calculations described next.) An actual physical model of the pathology might then be constructed using rapid-prototyping techniques,<sup>78,79</sup> and if the clinical circumstances permit, a patient-specific device could be tested on the physical model before actual clinical use. Next, if possible and if appropriate, a new biocompatible material will be selected so that the device can be absorbed once the desired intervention has been achieved, although reaching this goal may take longer than the envisioned time period. Finally, the basic manufacturing

process for generating the required functional elements of a new EIGI device will have to be further developed. For example, although it is doubtful that self-propelled yet tethered devices will be commercialized in 7–10 years, electrically activated shaped memory alloys (SMAs)<sup>80</sup> could be developed to supply the remote mechanical force needed for remote actuation. Functions, such as bending a guidewire or catheter to change its direction and guiding it into a desired vessel branch, could then be accomplished with more complex accommodations to the vessel geometry occurring when sealed catheter microjoints and robust electrical leads are developed. Alternatively for rotary motion, basic micro-machines that could be electrically activated would also have to be developed. Thus, rotational motion now used in cardiovascular applications for shaving plaque or for forming an intravascular ultrasound (IVUS) image could then be replaced with electrically activated rotating distal devices, which could be smaller and able to travel deeper into smaller vessels. Remote actuation would also enable IVUS for the neurovasculature, which is presently not possible because of the size and rigidity of current probes. Finally, although probably somewhat further into the future, there is the possibility for achieving very high spatial resolution using optical coherence tomography (OCT) imaging<sup>81</sup> if it can be applied intravascularly for viewing close to the surfaces of vessel lumens and endovascular devices. There is also the possibility of using nanotechnology for creating ultrasmall endovascular sensors (e.g., nanotube transistors for ionizing radiation measurement<sup>82</sup> and nanoavalanche photodiodes for photon detectors<sup>39</sup>) that might be used for guiding interventions.

### III.C. Procedure and treatment planning

**III.C.1. Prediction 5**—Treatment planning for EIGI procedures will be more extensive and involve simulations to verify the optimal selection of devices and equipment for delivery as well as flow calculations before, during, and after the intervention to check the intervention as it proceeds.

The rationale for this prediction is that as more detailed 3D morphological information about a vascular pathology becomes available from improved imaging studies and as computer power continues to increase in availability at reduced cost, the use of simulations has begun<sup>83</sup> and should naturally continue to blossom. Evidence for this happening in other areas, such as in radiation treatment planning, is apparent. Patient-specific dose delivery regimens and resulting distributions are computer simulated with clinical CT sequences as a basic part of the input data. For EIGI, however, there are two parts to a treatment plan that will have to be simulated: The device delivery based upon vessel morphology and mechanical device properties, and the blood flow results as determined using CFD calculations.

The implementation of increasingly sophisticated EIGI treatment plans will probably occur gradually. Current research into simulations for device transport through tortuous vasculature has begun; for example, with the tracking of a rigid stent of given dimensions and determining tolerances for passage along the parent vessel.<sup>53</sup> Increasingly sophisticated models<sup>84</sup> of the human vasculature, which include not only the morphology as derived from CT sequences for patients to be treated but also that of vessel flexibility and in the more distant future the inclusion of biological components to the model<sup>85</sup>—such as vessel wall cellular and molecular properties and constituents—will make treatment planning more accurate. There will be improved selection criteria for devices and delivery equipment as well as indications of potential vessel wall damage if nonoptimal deliveries must be made. The second important part of the EIGI treatment plan consisting of CFD simulation of the blood flow will depend upon continued progress being made in adapting the processes of solving the Navier–Stokes equation to the conditions of EIGIs and validating these results.<sup>86–90</sup> The verification link between actual blood flow situations, angiograms—where the flow of contrast media rather than blood is recorded, and CFD calculation results, must be accomplished. At present, this

validation process is being actively pursued using phantom experiments with both blood equivalent optical dye and denser more viscous radiographic contrast media.<sup>91,53</sup> Once there is confidence that the CFD results are valid, initial flow conditions established by MRA or ultrasound studies will be used together with the morphology determined by CBCT sequences as inputs to the CFD calculations. The treatment plan might then consist of simulating the deployment of a flow modifying device, such as a stent, for treatment of stenoses or the deployment of a specialized flow diverting stent<sup>92,87,93</sup> for treatment of aneurysms. Not only could velocity distributions and flow streamlines be simulated, but also wall shear stress—a possible predictor of pathology—could be estimated as well (Fig. 3).

As models get more sophisticated and computer power increases, it may be advantageous to do both the delivery and the CFD parts of the simulation almost in real time during the course of the EIGI to assist the interventionalist in making better decisions while the procedure is occurring. To further increase computer capability, it may be necessary to have a fast digital link to a super-computer facility to enable these complex calculations to be done so that actionable information is available during the EIGI.

### III.D. Personnel involved

**III.D.1. Prediction 6**—The medical physicist will take a more active role in individual clinical EIGI procedures as well as in the training of interventionalists using simulation systems.

If the future of EIGI procedures is as predicted herein, with more patient intensive treatment planning, the analogy of the medical physicist's role to that in radiation therapy treatment planning will be more plausible. As EIGI interventions become more technologically sophisticated, there will be a need for a professional clinical physicist to help in the selection of devices and delivery systems through simulations and quantitative analysis, as well as in overseeing the appropriate interpretation and use of CFD results for individual patient interventions. These responsibilities, of course, will be in addition to the primary continuing responsibility for the specification and quality assurance of all imaging systems.

Just as the therapy physicist is trained and certified in that branch of medical physics, the vascular medical physicist will have to be certified in EIGI physics as well. This implies the necessity for new or augmented curricula in medical physics training programs. While much of the basic hemodynamics and the CFD calculations may be presently in the domain of biomechanical engineers, we expect that future EIGI teams will consist of many medical professionals to enable this rapidly advancing field to reach its vast potential. However, it is our expectation that the vascular clinical medical physicist will be uniquely qualified to integrate the physics of imaging with the relevant aspects of biomechanical engineering involving interventional devices to be able to oversee the technical aspects of EIGI facilities as well as to head their scientific and engineering training programs for medical personnel. Not only will there be a new syllabus of EIGI physics related concepts to teach, but we expect that simulation-based training of the physicians<sup>94-99</sup> who perform EIGI procedures will become the standard. The interventionist will be able to practice and develop the necessary skills for catheter navigation and device deployment in a programmable simulated environment with tactile and visual feedback. The EIGI medical physicist with the collaboration of computer scientists will play a key role in both the use and the development of such systems.

## IV. Conclusions

In the 1966 movie *Fantastic Voyage*, there was an account of what future endovascular brain surgery could be like. It involved the shrinking of a submarine with a team of people that was injected into a patient and instructed to take a route through the vasculature to the brain to remove a blood clot in a vessel. While we do not quite predict such a capability, we believe



there will be considerable movement in the direction of miniaturization and remote actuation and guidance. We have made some specific forecasts regarding this rapidly advancing and exciting field of EIGI. We have predicted that imaging detectors will be markedly improved to better guide the use of newer and more complex interventional devices and delivery equipment using radiation more appropriately. We have described how we believe treatment planning for EIGI will be enhanced from the present rather informal qualitative planning to an increasingly sophisticated quantitative procedure, involving a new labor-intensive role for medical physicists somewhat akin to the role that medical physicists play in radiation treatment planning. Ultimately, we expect that advances in EIGI will lead to greatly improved patient procedures in which the medical physicist will play a crucial role.

## Acknowledgements

We thank the members of the University at Buffalo-Toshiba Stroke Research Center including Dr. Ciprian N. Ionita for supplying the angiographic images, Andrew Kuhls-Gilchrist for the SSXII image comparison, and Dr. Hui Meng's group for supplying the CFD images. The work was supported in part by the National Institutes of Health under Grant Nos. EB002873, NS43024, NS47242, HL52567, and EB02916, the National Science Foundation under Grant No. BES-0302389, the UB Interdisciplinary Research Development Fund (IRDF), and an equipment grant from Toshiba Medical Systems Corp.

## References

- Higashida RT, Lahue BJ, Torbey MT, Hopkins LN, Leip E, Hanley DF. Treatment of unruptured intracranial aneurysms: A nationwide assessment of effectiveness. *AJNR Am J Neuroradiol* 2007;28:146–151. [PubMed: 17213445]
- Koebbe CJ, Veznedaroglu E, Jabbour P, Rosenwasser RH. Endovascular management of intracranial aneurysms: current experience and future advances. *Neurosurgery* 2006;59:S3-93–S3-102.
- Koebbe CJ, Pandey A, Veznedaroglu E, Rosenwasser RH. The evolution and future directions of endovascular therapy. *Clin Neurosurg* 2006;53:191–195. [PubMed: 17380751]review
- Fiorella D, Woo HH. Emerging endovascular therapies for symptomatic intracranial atherosclerotic disease. *Stroke* 2007;38:2391–2396. [PubMed: 17585085]
- Saborowski O, Saeed M. An overview on the advances in cardiovascular interventional MR imaging. *Magn Reson Mater Phys Biol Med* 2007;20:117–127.
- Flamm SD. Cross-sectional imaging studies: What can we learn and what do we need to know. *Semin Vasc Surg* 2007;20:108–114. [PubMed: 17580248]
- Rauch, PL. Intravascular Brachytherapy Fluoroscopically Guided Interventions, AAPM Monograph No 28. AAPM, College Park; Maryland: 2002. A tour of the interventional vascular imaging suite; p. 547-616.
- Rowlands, JA.; Yorkston, J. Flat panel detectors for digital radiography. In: Beutel, J.; Kundel, HL.; Van Metter, RL., editors. *Handbook of Medical Imaging, Vol 1, Physics and Psychophysics*. SPIE; Bellingham, Washington: 2000. Chap. 4
- Bushberg, JT.; Siebert, JA.; Leidholdt, EM.; Boone, JM. *The Essential Physics of Medical Imaging*. Vol. 2nd. Lippincott Williams and Wilkins; Philadelphia, Pennsylvania: 2002. Fluoroscopy; p. 231-254. Chap 9
- Rudin S, Yadava G, Josan G, Kuhls A, Rangwala H, Wu Y, Ionita C, Bednarek DR. New light-amplifier-based detector designs for high spatial resolution and high sensitivity CBCT mammography. *Proc SPIE* 2006;6142:R1–R11.
- Granfors PR, Aufrichtig R, Possin GE, Giambattista BW, Huang ZS, Liu J, Ma B. Performance of a  $41 \times 41 \text{ cm}^2$  amorphous silicon flat panel x-ray detector designed for angiographic and R&F imaging applications. *Med Phys* 2003;30:2715–2726. [PubMed: 14596310]
- Bloomquist AK, Yaffe MJ, Mawdsley GE, Hunter DM, Beideck DJ. Lag and ghosting in a clinical flat-panel selenium digital mammography system. *Med Phys* 2006;33:2998–3005. [PubMed: 16964878]
- Siewerdsen JH, Jaffray DA. A ghost story: Spatio-temporal response characteristics of an indirect-detection flat-panel imager. *Med Phys* 1999;26:1624–1641. [PubMed: 10501063]

14. Schmidgunst C, Ritter D, Lang E. Calibration model of a dual gain flat panel detector for 2D and 3D x-ray imaging. *Med Phys* 2007;34:3649–3666. [PubMed: 17926969]
15. Ganguly A, Rudin S, Bednarek DR, Hoffmann KR, Kyprianou I. Micro-angiography for neurovascular imaging, Part 1: Experimental measurements and feasibility. *Med Phys* 2003;30:3018–3028. [PubMed: 14655949]
16. Food and Drug Administration, FDA Public Health Advisory. Center for Devices and Radiological Health; Rockville, Maryland: [September 30, 1994]. Avoidance of serious x-ray induced skin injuries to patients during fluoroscopically-guided procedures. available at <http://www.fda.gov/cdrh/fluor.html>
17. Wagner LK, McNeese MD, Marx MV, Siegel EL. Severe skin reactions from interventional fluoroscopy: Case report and review of the literature. *Radiology* 1999;213:773–776. [PubMed: 10580952]
18. Rudin S, Bednarek DR. Region of interest fluoroscopy. *Med Phys* 1992;19:1183–1189. [PubMed: 1435596]
19. Rudin S, Bednarek DR, Guterman LR, Wakhloo A, Hopkins LN, Fletcher L, Massoumzadeh P. Implementation of region of interest fluoroscopy using the road mapping mode of a real-time digital radiographic unit. *Radiographics* 1995;15:1465–1470. [PubMed: 8577969]
20. Rudin S, Guterman LR, Granger W, Bednarek DR, Hopkins LN. Neuro-interventional radiologic application of region of interest (ROI) imaging techniques. *Radiology* 1996;199:870–873. [PubMed: 8638020]
21. Rudin S, Bednarek DR, Kezerashvili M, Granger W, Serghany J, Guterman LR, Hopkins LN, Massoumzadeh P, Szymanski B, Loftus R. Clinical application of region of interest (ROI) radiologic imaging techniques. *Radiographics* 1996;16:895–902. [PubMed: 8835978]
22. Gkanatsios NA, Huda W, Peters KR, Freeman JA. Evaluation of an on-line patient exposure meter in neuroradiology. *Radiology* 1997;203:837–842. [PubMed: 9169713]
23. Balter, S.; Fletcher, DW.; Kuan, HM.; Miller, D.; Richter, D.; Seissl, H.; Shope, TB. Techniques to estimate radiation dose to skin during fluoroscopically guided procedures. In: Balter, S.; Chan, R.; Shope, T., editors. *Intravascular Brachytherapy/Fluoroscopically-Guided Interventions*. AAPM Summer School Proceedings; Madison, Wisconsin: 2002. p. 731-764.
24. Dotter CT, Judkins MP. Transluminal treatment of arteriosclerotic obstruction. Description of a new technic and a preliminary report of its application, 1964. *Radiology* 1989;172:904–920. [PubMed: 2528161]classical article
25. Ceschinski H, Henkes H, Weinert HC, Weber W, Kuhne D, Monstadt H. Torquability of microcatheter guidewires: the resulting torsional moment. *Biomed Mater Eng* 2000;10:31–42. [PubMed: 10950205]
26. Carey J, Fahim A, Munro M. Design of braided composite and cardiovascular catheters based on required axial, flexural and torsional rigidities. *J Biomed Mater Res, Part B: Appl Biomater* 2004;70B:73–81. [PubMed: 15199586]
27. Carey J, Emery D, McCracken P. Buckling test as a new approach to testing flexural rigidities of angiographic catheters. *J Biomed Mater Res, Part B: Appl Biomater* 2006;76B:211–218. [PubMed: 16080187]
28. Bloss P, Rothe W, Wunsche P, Werner C, Rothe A, Kneissl GD, Burger W, Rehberg E. Investigations of the pushability behavior of cardiovascular angiographic catheters. *Biomed Mater Eng* 2003;13:327–343. [PubMed: 14646048]
29. Zoarski GH, Mathis JM, Hebel JR. Performance characteristics of microcatheter systems in a standard tortuous pathway. *AJNR Am J Neuroradiol* 1998;19:1571–1576. [PubMed: 9763396]
30. Anderson JM. The future of biomedical materials. *J Mater Sci Mater Med* 2006;17:1025–8. [PubMed: 17122914]review
31. Kim, SH.; Campanella, BA.; Qureshi, AI.; Ringer, AJ.; Boulos, AS.; Lopes, DK.; Guterman, LR.; Hopkins, LN. Management of Cerebral Aneurysms. Le Roux, PD.; Winn, HR.; Newell, DW., editors. Saunders; Philadelphia: 2004. p. 883-902.
32. Ginete, WL. Rotational Atherectomy: Current Perspectives. [www.med.umn.edu/img/assets/7172/Rotational\\_Atherectomy\\_073004.swf](http://www.med.umn.edu/img/assets/7172/Rotational_Atherectomy_073004.swf)

33. Bevan, JA.; Kaley, G.; Rubanyi, GM., editors. Flow-Dependent Regulation of Vascular Function. Oxford University Press; New York: 1995.
34. Davies PF, Spaan JA, Krams R. Shear stress biology of the endothelium. *Ann Biomed Eng*, Special Issue: International Biofluid Mechanics Symposium 2005;33(12):1714–1718.
35. Imbesi SG, Kerber CW. Analysis of slipstream flow in a widened-necked basilar artery aneurysm: Evaluation of potential treatment regimens. *AJNR Am J Neuroradiol* 2001;22:721–724. [PubMed: 11290486]
36. Wakhloo AK, Lieber BB, Seong J, Sadasivan C, Gounis MJ, Miskolczi L, Sandhu JS. Hemodynamics of carotid artery atherosclerotic occlusive disease. *J Vasc Interv Radiol* 2004;15:S111–21. [PubMed: 15101520]review
37. Vedantham S, Karellas A, Suryanarayanan S. Solid-state fluoroscopic imager for high resolution angiography. Physical characteristic of an 8 cm×8 cm experimental prototype. *Med Phys* 2004;31:1462–1472. [PubMed: 15259649]
38. Hunt DC, Tanioka K, Rowlands JA. X-ray imaging using avalanche multiplication in amorphous selenium: investigation of depth dependent avalanche noise. *Med Phys* 2007;34:976–986. [PubMed: 17441244]
39. Hayden O, Agarwal R, Lieber CM. Nanoscale avalanche photodiodes for highly sensitive and spatially resolved photon detection. *Nat Mater* 2006;5:352–356. [PubMed: 16617344]
40. Zhao W, Li D, Reznik A, Lui B, Hunt DC, Tanioka K, Rowlands JA. Indirect flat-panel detector with avalanche gain: design and operation of the avalanche photoconductor. *Proc SPIE* 2005;5745:352–360.
41. Izadi MH, Karim KS, Nathan A, Rowlands JA. Low-noise architecture for advanced diagnostic medical x-ray imaging applications. *Proc SPIE* 2006;6142:T1–T11.
42. Taghibakhsh F, Karim KS. Amplified pixel sensor architectures for low dose computed tomography using silicon thin film technology. *Proc SPIE* 2007;6510:W1–W8.
43. Hyneczek J. Impactron—A new solid state image intensifier. *IEEE Trans Electron Devices* 2001;48:2238–2241.
44. Robbins MS, Hadwen BJ. The noise performance of electron multiplying charge-coupled devices. *IEEE Trans Electron Devices* 2003;50:1227–1232.
45. Kuhls AT, Yadava G, Patel V, Bednarek DR, Rudin S. Progress in electron-multiplying CCD (EMCCD) based, high-resolution, high-sensitivity x-ray detector for fluoroscopy and radiography. *Proc SPIE* 2007;6510:C1–C11.
46. Cunningham, IA. Applied linear systems theory. In: Beutel, J.; Kundel, HL.; Van Metter, RL., editors. *Handbook of Medical Imaging, Vol 1. Physics and Psychophysics*. SPIE; Bellingham, Washington: 2000. Chap. 2
47. Ganguly A, Rudin S, Bednarek DR, Hoffmann KR. Micro angiography for Neuro vascular imaging, part 2: Cascade model analysis. *Med Phys* 2003;30:3029–3039. [PubMed: 14655950]
48. Kyprianou I, Rudin S, Bednarek DR, Hoffmann KR. Generalizing the MTF and DQE to include x-ray scatter and focal spot unsharpness: Application to a new micro-angiographic system for clinical use. *Med Phys* 2005;32:613–626. [PubMed: 15789608]
49. Yadava GK, Kyprianou IS, Rudin S, Bednarek DR, Hoffmann KR. Generalized performance evaluation of x-ray image intensifier compared with a microangiographic system. *Proc SPIE* 2005;5745:419–429.
50. Siemens iPilot, Axiom No. 2, March, 2006, pp. 10–17, pamphlet from Siemens Medical Corp.. [http://www.medical.siemens.com/siemens/sv\\_SE/rg\\_marcom\\_FBAs/files/brochures/magazin\\_archive\\_ax/AXIOM\\_Innovati](http://www.medical.siemens.com/siemens/sv_SE/rg_marcom_FBAs/files/brochures/magazin_archive_ax/AXIOM_Innovati)
51. Philips Xpervision Newsletter. [November, 2006]. [http://www.medical.philips.com/us/products/cardiovascular/assets/docs/XperVision\\_Newsletter\\_int.pdf](http://www.medical.philips.com/us/products/cardiovascular/assets/docs/XperVision_Newsletter_int.pdf)
52. Chityala R, Hoffmann KR, Bednarek DR, Rudin S. Region of interest (ROI) computed tomography (CT): comparison with full field of view (FFOV) and truncated CT for a human head phantom. *Proc SPIE* 2005;5745:583–590.
53. Hoffmann, KR.; Rudin, S.; Meng, H.; Hopkins, LN.; Guterman, L.; Levy, E. Multidimensional Image Processing, Analysis, and Display. Armato, SG.; Brown, MS., editors. *RSNA*; Oak Brook, Illinois: 2005. p. 173-184.

54. Schafer S, Singh V, Hoffmann KR, Noël PB, Xu J. Planning image-guided endovascular interventions: guidewire simulation using shortest path algorithms. *Proc SPIE* 2007;6509:C1–C10.
55. International Electrotechnical Commission. Report 60601–2-43, Medical electrical equipment Part 2-43: Particular requirements for the safety of x-ray equipment for interventional procedures. Geneva, Switzerland: 2000.
56. U. S. Food and Drug Administration (FDA). HHS: Electronic Products–Federal performance standard for diagnostic x-ray systems and their major components, Federal Register June 10;2005 70(Number 111):33997–34042.
57. Massoumzadeh P, Rudin S, Bednarek DR. Filter material selection for region of interest radiologic imaging. *Med Phys* 1998;25:161–171. [PubMed: 9507475]
58. Dinu PM, Bednarek DR, Wobschall D, Peterson R, Ionita CN, Rudin S, Zeng M, Chugh K, Hoffmann KR. X-ray beam tracking system for a fluoroscopic c-arm unit. *Med Phys* 2003;30:1424.
59. Chugh K, Dinu PM, Bednarek DR, Wobschall D, Rudin S, Hoffmann KR, Peterson R, Zeng M. A computer-graphic display for real-time operator feedback during interventional x-ray procedures. *Proc SPIE* 2004;5367:464–473.
60. Food and Drug Administration, Important Information for Physicians and other Health Care Professionals. Center for Devices and Radiological Health; Rockville Maryland: [September 15, 1995]. Recording information in the patient's medical record that identifies the potential for serious x-ray-induced skin injuries following fluoroscopically-guided procedures. available at <http://www.fda.gov/cdrh/xrayinj.html>
61. Miller DL, Balter S, Wagner LK, Cardella J, Clark TW, Neithamer CD Jr, Schwartzberg MS, Swan TL, Tobwin RB, Rholl KS, Sacks D. SIR standards of Practice Committee. Quality improvement guidelines for recording patient radiation dose in the medical record. *J Vasc Interv Radiol* 2004;15:423–429. [PubMed: 15126651]
62. Wagner, LK. Intravascular Brachytherapy / Fluoroscopically-Guided Interventions. Balter, S.; Chan, R.; Shope, T., editors. AAPM Summer School Proceedings; Madison, Wisconsin: 2002. p. 195-218.
63. Ormiston JA, Webster MWI, Armstrong G. First-in-human implantation of a fully bioabsorbable drug-eluting stent: the BVS poly-L-lactic acid everolimus eluting coronary stent. *Catheter Cardiovasc Interv* 2007;69:128–131. [PubMed: 17139655]
64. Erbel R, et al. Temporary scaffolding of coronary arteries with bioabsorbable magnesium stents: a prospective, non-randomised multicentre trial. *Lancet* 2007;369:1869–1875. [PubMed: 17544767]
65. Ormiston J, Webster M. Absorbable coronary stents. *Lancet* 2007;369:1839–1840. [PubMed: 17544749]comment
66. Saito S. New horizon of bioabsorbable stent. *Catheter Cardiovasc Interv* 2005;66:595–596. [PubMed: 16284981]commenteditorial
67. <http://www.stereotaxis.com/>
68. Armacost MP, Adair J, Munger T, Viswanathan R, Creighton FM, Curd DT, Sehra R. Accurate and reproducible target navigation with the stereotaxis Niobe Magnetic Navigation System. *J Cardiovasc Electrophysiol* 2007;18:S26–S31.
69. Pappone C, et al. Robotic magnetic navigation for atrial fibrillation ablation. *J Am Coll Cardiol* 2006;47:1390–1400. [PubMed: 16580527]
70. Florin E, Rangwala HS, Rudin S. Method to rotate an endovascular device around the axis of a vessel using an external magnetic field. *Med Phys* 2007;34:328–333. [PubMed: 17278518]
71. Settecase F, Sussman MS, Wilson MW, Hetts S, Arenson RL, Malba V, Bernhardt AF, Kucharczyk W, Roberts TPL. Magnetically-assisted remote control (MARC) steering of endovascular catheters for interventional MRI: A model for deflection and design implications. *Med Phys* 2007;34:3135–3142. [PubMed: 17879774]
72. <http://www.hansenmedical.com/products/sensei.aspx>
73. Al-Ahmad AD, Grossman J, Wang PJ. Early experience with a computerized robotically controlled catheter system. *J Interv Card Electrophysiol* 2005;12:199–202. [PubMed: 15875110]
74. Cercenelli L, Marcelli E, Plicchi G. Initial experience with a telerobotic system to remotely navigate and automatically reposition standard steerable EP catheters. *ASAIO J* 2007;53:523–529. [PubMed: 17885323]

75. Buckley PR, McKinley GH, Wilson TS, Small W IV, Bennett WJ, Beringer JP, McElfresh MW, Maitland DJ. Inductively heated shape memory polymer for the magnetic actuation of medical devices. *IEEE Trans Biomed Eng* 2006;53:2075–2083. [PubMed: 17019872]
76. Nesbit GM, Luh G, Tien R, Barnwell SL. New and future endovascular treatment strategies for acute ischemic stroke. *J Vasc Interv Radiol* 2004;15:S103–S110. [PubMed: 15101519]
77. Wood BJ, Locklin JK, Viswanathan A, Kruecker J, Haemmerich D, Cebral J, Sofer A, Cheng R, McCreedy E, Cleary K, McAuliffe MJ, Glossop N, Yanof J. Technologies for guidance of radiofrequency ablation in the multimodality interventional suite of the future. *J Vasc Interv Radiol* 2007;18:9–24. [PubMed: 17296700]review
78. Seong J, Sadasivan C, Onizuka M, Gounis MJ, Christian F, Miskolczi L, Wakhloo AK, Lieber BB. Morphology of elastase-induced cerebral aneurysm model in rabbit and rapid prototyping of elastomeric transparent replicas. *Biorheology* 2005;42:345–361. [PubMed: 16308466]
79. Sherman JR, Rangwala HS, Ionita CN, Dohatcu AC, Bednarek DR, Hoffmann KR, Rudin S. Investigation of new flow modifying endovascular image-guided interventional (EIGI) techniques in patient specific aneurysm phantoms (PSAPs) using optical imaging. *Proc SPIE*. in press
80. Kohl, M. *Shape Memory Microactuators*. Springer; New York: 2004.
81. Fujimoto, JG. M. I. T. Research, Laboratory of Electronics (RLE). PI, <http://www.rle.mit.edu/rleonline/research/LaserMedicineandMedicalImagingGroup.html>
82. Tang XW, Yang Y, Kim W, Wang Q, Qi P, Dai H, Xing L. Measurement of ionizing radiation using carbon nanotube field effect transistor. *Phys Med Biol* 2005;50:N23–N31. [PubMed: 15773731]
83. Karmonik C, Strother CM, Chen X, Deinzer F, Klucznik R, Mawad ME. Stent-assisted coiling of intracranial aneurysms aided by virtual parent artery reconstruction. *AJNR Am J Neuroradiol* 2005;26:2368–2370. [PubMed: 16219847]
84. Baráth K, Cassot F, Rüfenacht DA, Fasel JHD. Anatomically shaped internal carotid artery aneurysm *in vitro* model for flow analysis to evaluate stent effect. *AJNR Am J Neuroradiol* 2004;25:1750–1759. [PubMed: 15569741]
85. Baek S, Rajagopla KR, Humphrey JD. A theoretical model of enlarging intracranial fusiform aneurysms. *J Biomech Eng* 2006;128:142–149. [PubMed: 16532628]
86. Ford MD, Stuhne GR, Nikolov HN, Habets DF, Lownie SP, Holdsworth DW, Steinman DA. Virtual angiography for visualization and validation of computational models of aneurysm hemodynamics. *IEEE Trans Med Imaging* 2005;24:1586–1592. [PubMed: 16350918]
87. Kim M, Ionita CN, Tranquebar RV, Hoffmann KR, Taulbee DB, Meng H, Rudin S. Evaluation of an asymmetric stent patch design for a patient specific intracranial aneurysm using computational fluid dynamic (CFD) calculations in the computed tomography (CT) derived lumen. *Proc SPIE* 2006;6143:G1–G8.
88. Cebral JR, Pergolizzi RS Jr, Putnam CM. Computational fluid dynamics model of intracranial aneurysms: qualitative comparison with cerebral angiography. *Acad Radiol* 2007;14:804–813. [PubMed: 17574131]
89. Cebral J, Radaelli A, Frangi A, Putman C. Hemodynamics before and after bleb formation in cerebral aneurysms. *Proc SPIE* 2007;6511:65112C1–65112C9.
90. Appanaboyina S, Mut F, Löhner R, Putman C, Cebral J. Patient specific modeling of intracranial aneurysmal stenting. *Proc SPIE* 2007;6511:65112D1–65112D11.
91. Wang Z, Ionita CN, Rudin S, Hoffmann KR, Paxton AB, Bednarek DR. Angiographic analysis of blood flow modification in cerebral aneurysm models with a new asymmetric stent. *Proc SPIE* 2004;5369:307–318.
92. Rudin S, Wang Z, Kyprianou I, Hoffmann KR, Wu Y, Meng H, Guterman LR, Nemes B, Bednarek DR, Dmochowski J, Hopkins LN. Measurement of flow modification in phantom aneurysm model: comparison of coils and a longitudinally and axially asymmetric stent-initial findings. *Radiology* 2004;231:272–276. [PubMed: 15068953]
93. Lieber, BB.; Sadasivan, C.; Miskolczi, L.; Cesar, L.; Seong, J.; Wakhloo, AK. Flow divertors to treat cerebral aneurysms: preliminary results in the rabbit elastase-induced aneurysm model. *Proceedings BIO2006, ASME 2006 Summer Bioengineering Conference; June 21–25, 2006; Amelia Island Plantation, Amelia Island, Florida.*

94. Alderliesten T, Konings MK, Niessen WJ. Simulation of minimally invasive vascular interventions for training purposes. *Comput Aided Surg* 2004;9:3–15. [PubMed: 15792932]
95. Alderliesten T, Konings MK, Niessen WJ. Modeling friction, intrinsic curvature, and rotation of guidewires for simulation of minimally invasive vascular interventions. *IEEE Trans Biomed Eng* 2007;54:29–39. [PubMed: 17260853]
96. Duriez C, Cotin S, Lenoir J, Neumann P. New approaches to catheter navigation for interventional radiology simulation. *Comput Aided Surg* 2006;11:300–308. [PubMed: 17458764]
97. Dawson DL. Training in carotid artery stenting: Do carotid simulation systems really help? *Vascular* 2006;14:256–263. [PubMed: 17038295]review
98. Gould DA, Kessel DO, Healey AE, Johnson SJ, Lewandowski WE. Simulators in catheter-based interventional radiology: training or computer games? *Clin Radiol* 2006;61:556–561. [PubMed: 16784940]reviewGould DA, Kessel DO, Healey AE, Johnson SJ, Lewandowski WE. *Clin Radiol* 2006;61:903.erratum
99. Sengupta A, Kesavadas T, Hoffmann KR, Baier RE, Schafer S. Evaluating tool-artery interaction force during endovascular neurosurgery for developing haptic engine. *Stud Health Technol Inform* 2007;125:418–420. [PubMed: 17377315]

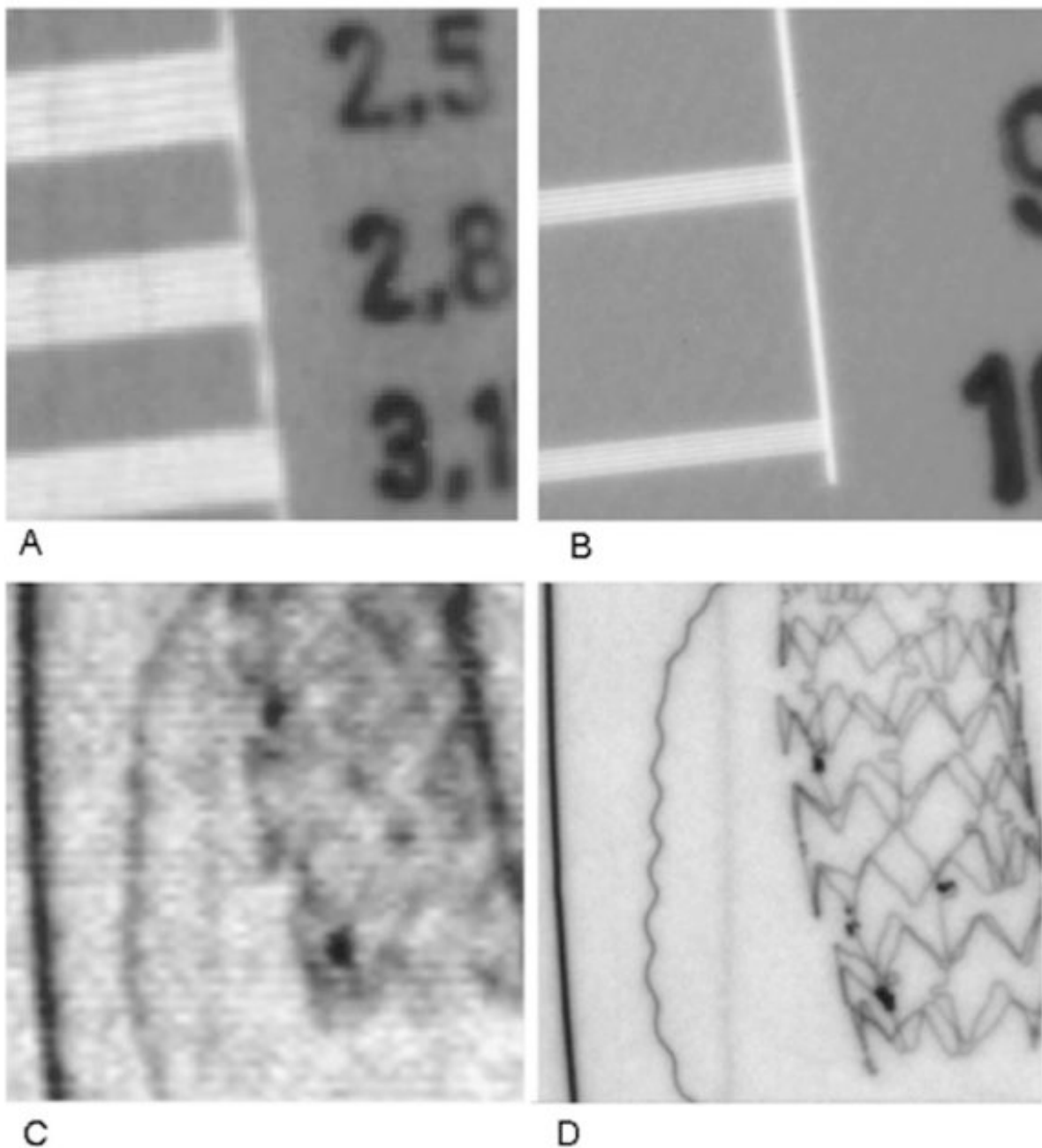


**Fig. 1.**

Improved resolution with new SSXII (right) compared with XII (left). (A) and (B) Bar pattern images taken at 70 kVp with 2 in. PMMA filtration added with the same exposure for each detector. (C) and (D) Images of a neurovascular phantom containing thin wires (left to right: 100  $\mu\text{m}$  Au, 25  $\mu\text{m}$  Cu, 50  $\mu\text{m}$  Pt), 100  $\mu\text{m}$  iodine contrast media-filled tube and a new asymmetric vascular stent having a blood flow diverting low-porosity polyurethane patch (indicated by four Pt markers) designed for closing off flow into an aneurysm were taken at 74 kVp with 21.4 mm Al added filtration (RQA 5 Spectrum) with the same exposure. (A) Bar pattern with only 3.1 Lp/mm visible for XII in 5 in. magnification mode. (B) Bar pattern with 10 Lp/mm clearly visible for SSXII. (C) With the XII, wires are less clear: Cu wire and Pt wire

bends are unseen and stent struts and patch markers are not clearly visible. (D) With the SSXII, Cu wire is barely visualized but Pt wire bends and stent struts and patch markers are clearly visible.



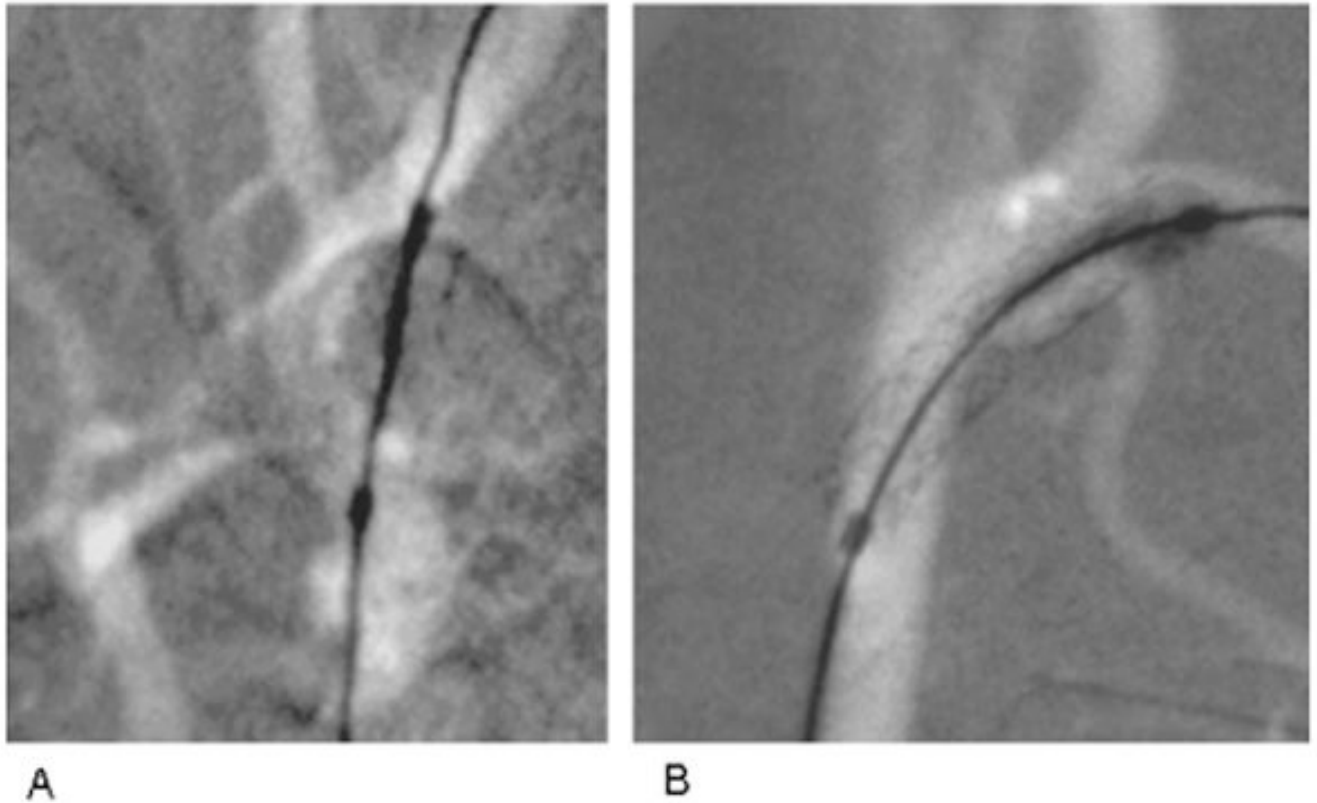


**Fig. 2.** Fluoroscopic road-mapped frames done at 74 kVp and 50 mA of 3 mm diameter and 15 mm long coronary stent systems (Multi-link Vision, Guidant Corp, Santa Clara, CA). End markers indicate extent of expanded balloon on delivery catheter. Stents are deployed in carotid arteries of the same rabbit. (A) Using 2 ms pulsed XII imaging with temporal filtering (standard on commercial systems), stent deployed in right carotid. (B) Using 8 ms pulsed HSMAF imaging with no temporal filtering, stent deployed in left carotid showing improved visualization of details of stent struts and vessel edges.

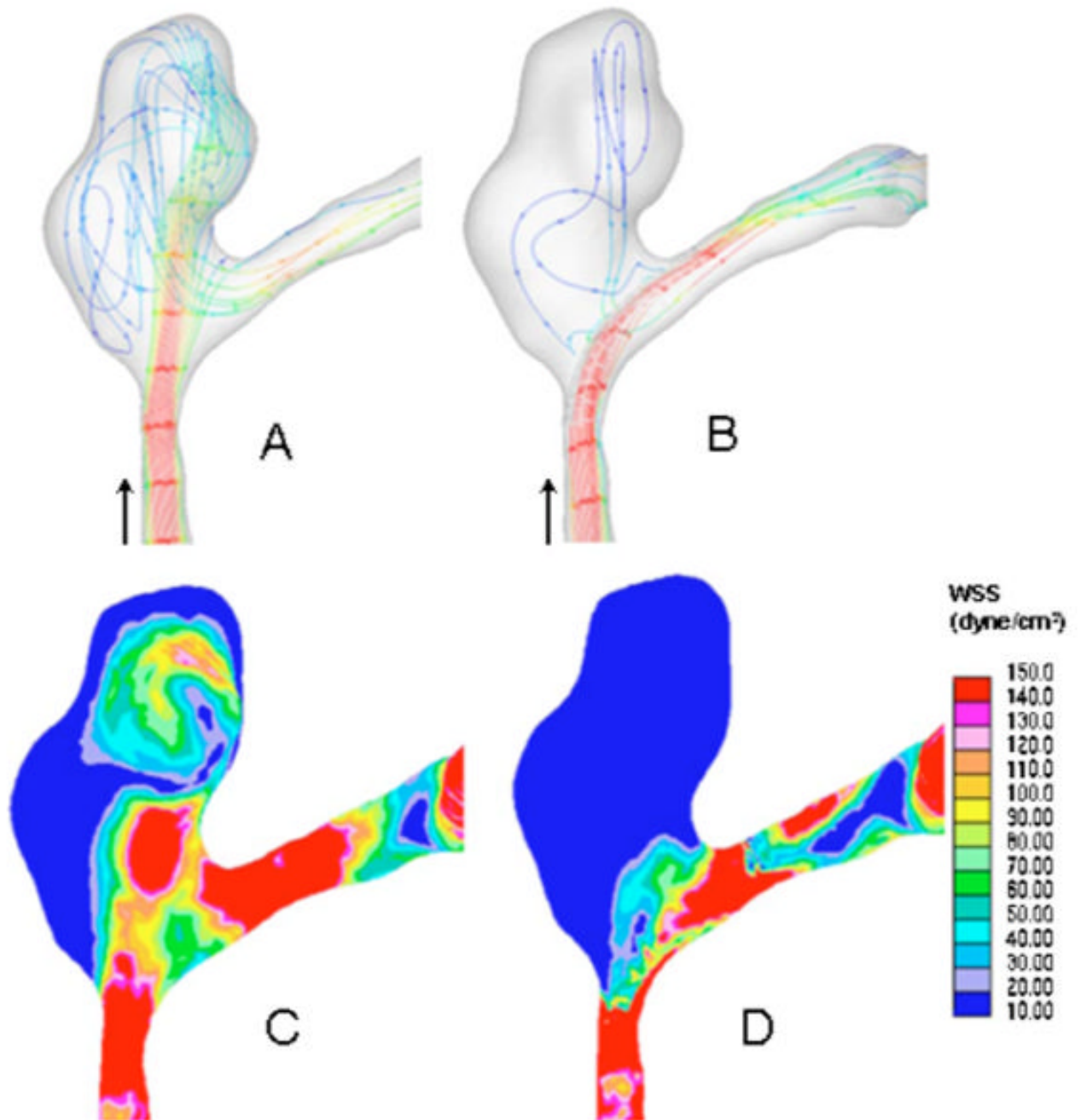


**Fig. 3.** CFD result showing streamlines and local shear stress distributions for a patient-specific aneurysm untreated and treated with an asymmetric vascular stent (Ref. 87). Notice effect of flow diversion on streamlines and wall shear stress (WSS) distribution. (A) Streamlines, untreated; (B) streamlines, treated; (C) wall shear stress, untreated; (D) wall shear stress, treated.